

# Journal of Materials Chemistry C

Accepted Manuscript



This is an *Accepted Manuscript*, which has been through the Royal Society of Chemistry peer review process and has been accepted for publication.

*Accepted Manuscripts* are published online shortly after acceptance, before technical editing, formatting and proof reading. Using this free service, authors can make their results available to the community, in citable form, before we publish the edited article. We will replace this *Accepted Manuscript* with the edited and formatted *Advance Article* as soon as it is available.

You can find more information about *Accepted Manuscripts* in the [Information for Authors](#).

Please note that technical editing may introduce minor changes to the text and/or graphics, which may alter content. The journal's standard [Terms & Conditions](#) and the [Ethical guidelines](#) still apply. In no event shall the Royal Society of Chemistry be held responsible for any errors or omissions in this *Accepted Manuscript* or any consequences arising from the use of any information it contains.

Cite this: DOI: 10.1039/c0xx00000x

www.rsc.org/xxxxxx

ARTICLE TYPE

## Layer-by-Layer Self-assembly Films for Building Magnetic Driven Walking Devices

Hong-Su Zhang,<sup>a</sup> Ling Luo,<sup>a</sup> Ge Fang,<sup>b</sup> Wan-Zhen Zhang,<sup>a</sup> Bang-Jing Li,<sup>\*b</sup> Sheng Zhang,<sup>\*a</sup>

Received (in XXX, XXX) Xth XXXXXXXXX 20XX, Accepted Xth XXXXXXXXX 20XX

DOI: 10.1039/b000000x

In this paper, we fabricated a magnetic-driven walking device comprising magnetic active layer-by-layer films. Alternating the magnetic fields, the device walked steadily and fast on the substrate like an inchworm, and showed good transportation capability.

In recent years, much attention has been focused on designing soft polymeric actuators for the realization of biomimetic movements and micro-robot walking. Stimuli-responsive soft polymeric materials, which can control two- or three-dimensional shape changes in response to external stimuli, are of key importance in fabricating soft actuators. Although various stimuli-responsive soft materials, such as gels and elastomers,<sup>1</sup> have been developed, their functionality as robotic actuators has not been largely explored. A few devices driven by molecular motors, electric fields, light, temperature, and humidity have been developed.<sup>2-6</sup> But to address the demand of operating the device in wide range of environmental conditions and controlling the device easily, noncontact driven methods are expected. Up to now, the main remote energy to power the actuators is light, which is converted into mechanical motion without the need for direct contact to the actuator.<sup>4</sup> However, the response of many light-driven actuators is relatively slow. Magnetic driven is another alternative approach to realize mechanical motion. The magnet powering devices have potential advantages, like more robustness, and faster response times. Herein we report a magnetic active device capable of walking and transporting cargo.

Magnetically active, soft polymers are typically based on composites consisting of magnetic particles dispersed in a polymer matrix. They have application in information storage, magnetic imaging, medicine, etc.<sup>7</sup> However, their functionality as actuators for motion devices is seldomly explored.<sup>8</sup> In this study, we prepare a kind of flexible magnetic film as an actuator, which bends periodically, walks on a ratchet substrate and carry the cargo under periodic magnetic field.

So far, several techniques have been developed to fabricate the magnetic films, such as vacuum evaporation, sputtering, electrophoresis, pulse laser deposition, Langmuir-Blodgett (LB) deposition, and layer-by-layer (LBL) assembly etc.<sup>9</sup> We build the magnetic actuator (a free-standing magnetic film) using LBL methods because of its simplicity and universality. The process can be described as the sequential adsorption of layers of magnetic particles on oppositely charged layers of

polyelectrolytes. Superparamagnetic Fe<sub>3</sub>O<sub>4</sub> and polyanion alginate (Alg) are used as building blocks.

Kotov et al. ever reported the preparation of free-standing LBL film composed of Fe<sub>3</sub>O<sub>4</sub> nanoparticles and oppositely charged polyelectrolytes.<sup>9g</sup> In this study, the Fe<sub>3</sub>O<sub>4</sub> are encapsulated into positive ion hollow microparticles firstly in order to achieve more homogenous film and circumvent the leaching of nanomagnet from film during use as an actuator.

In our previous report, we have developed an approach to construct hollow microparticles by formation coil-rod inclusion complex between cyclodextrin (CD) and block copolymer.<sup>10</sup> These hollow particles could encapsulate enzyme, gene, or magnetofluids during the self-assembly process.<sup>11</sup> Here, polyethylenimine-*b*-poly(ethylene glycol) (PEI-PEG) copolymer is selected for the preparation of hollow microspheres.

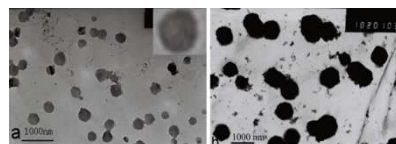


Fig. 1 TEM micrographs of nanospheres: (a) PEG-PEI/ $\alpha$ -CD. (b) PEG-PEI/ $\alpha$ -CD/Fe<sub>3</sub>O<sub>4</sub>.

As demonstrated in our previous work,<sup>11d</sup> the  $\alpha$ -CDs exclusively threaded on the PEG segment to form a rod block and the PEI segment acted as a coil block. The requirement of efficient space-filling packing of the rod-like block resulted in the PEG- $\alpha$ -CD inclusions preferring the pack radially into a sphere to form a hollow structure. The expected structure of such a particle was inner PEG- $\alpha$ -CD inclusion blocks surround by coil-like PEI shell. Transmission electron microscopy (TEM) images revealed that most PEI-PEG/ $\alpha$ -CD particles showed a contrast between the gray center and the dark periphery (Fig. 1a), which was typical TEM image of hollow particle.<sup>11</sup> The Fe<sub>3</sub>O<sub>4</sub> were easily entrapped into the empty domain of PEI-PEG/ $\alpha$ -CD particles while the particles were formed. Fig. 1b showed the morphology of the PEI-PEG/ $\alpha$ -CD/Fe<sub>3</sub>O<sub>4</sub> studied by TEM. It can be seen that the particles were dark and no bright domains can be found, suggesting that the presence of magnetofluids had no effect of the self-assembly procedure and the particles were filled with Fe<sub>3</sub>O<sub>4</sub>. The size of PEI-PEG/ $\alpha$ -CD/Fe<sub>3</sub>O<sub>4</sub> particles was about 700-900 nm. The zeta potential of PEI-PEG/ $\alpha$ -CD/Fe<sub>3</sub>O<sub>4</sub> particles was 44.8 mV, confirming that the surface of the particles was covered by protonated PEI blocks. The IR spectra of PEI-PEG/ $\alpha$ -CD and

PEI-PEG/ $\alpha$ -CD/ $\text{Fe}_3\text{O}_4$  were quite similar, suggesting that there were not big interactions between the  $\text{Fe}_3\text{O}_4$  fillers and the polymer shells. (Figure S4)

The PEI-PEG/ $\alpha$ -CD/ $\text{Fe}_3\text{O}_4$  particles were positively charged and therefore were electrostatically attracted to negatively charged Alg layer. A traditional LBL process of sequentially coating a surface with layers of PEI-PEG/ $\alpha$ -CD/ $\text{Fe}_3\text{O}_4$  particles and Alg by immersing a cellulose acetate (CA) substrate in dilute solutions of the components was used in this study. After 100 deposition cycles, the CA substrate was easy peeled off by immersing the film in acetone for 48 h. The obtained free-standing film was brown and showed high uniformity, strength and flexibility (Fig. 2a). The cross-sectional scan electron microscopy (SEM) image of the Alg/(PEI-PEG/ $\alpha$ -CD/ $\text{Fe}_3\text{O}_4$ ) film provided thickness measurements of 85  $\mu\text{m}$  for 100-bilayer films (Fig. S5). Therefore, the thickness of per bilayer was around 850 nm, which coincided with the diameter of PEI-PEG/ $\alpha$ -CD/ $\text{Fe}_3\text{O}_4$  particles. It should be noticed that in this cross-sectional SEM, we can not observed the distribution of particles. As Kotov et al. ever reported that in many instances the layered nature of the films is obscured by interpenetration of the subsequent layers and high interlayer roughness.<sup>9b</sup> This result also implied that the PEI-PEG/ $\alpha$ -CD/ $\text{Fe}_3\text{O}_4$  particles did not aggregate. The fracture surface of Alg/(PEI-PEG/ $\alpha$ -CD/ $\text{Fe}_3\text{O}_4$ ) film was pretty rough, indicating that this film exhibited ductile fracture.

Measurement of mechanical properties also confirmed that the Alg/(PEI-PEG/ $\alpha$ -CD/ $\text{Fe}_3\text{O}_4$ ) film was typical ductile material. The stress-strain curve of Alg/(PEI-PEG/ $\alpha$ -CD/ $\text{Fe}_3\text{O}_4$ ) film showed that this material exhibited large strains and yielding before it failed. (Figure S6)

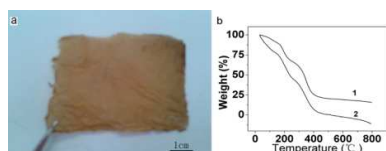


**Fig. 2** (a) Images of free-standing Alg/(PEI-PEG/ $\alpha$ -CD/ $\text{Fe}_3\text{O}_4$ ) film. (b) TGA thermograms of (1) free-standing (Alg/(PEI-PEG/ $\alpha$ -CD/ $\text{Fe}_3\text{O}_4$ ) film and (2) free-standing Alg/(PEI-PEG/ $\alpha$ -CD) film.

Thermogravimetric analysis (TGA) was carried out to determine the magnetofluids content of the Alg/(PEI-PEG/ $\alpha$ -CD/ $\text{Fe}_3\text{O}_4$ ) film. As shown in Fig. 2b, the film without  $\text{Fe}_3\text{O}_4$  lost 100 % weight at 500  $^\circ\text{C}$ , while the film with  $\text{Fe}_3\text{O}_4$  only lost 79.6 % weight. As TGA yields an organic weight fraction of Alg- $\text{Fe}_3\text{O}_4$  film, the content of magnetofluids of the Alg/(PEI-PEG/ $\alpha$ -CD/ $\text{Fe}_3\text{O}_4$ ) film was about 20.4 wt%.



**Fig. 3** Bending and stretching movements of free-standing Alg/(PEI-PEG/ $\alpha$ -CD/ $\text{Fe}_3\text{O}_4$ ) film with changing the placement of permanent magnet.

We compared the uniformity of Alg/(PEI-PEG/ $\alpha$ -CD/ $\text{Fe}_3\text{O}_4$ ) and Alg/ $\text{Fe}_3\text{O}_4$  film prepared by casting method. It was found that the standard deviations of the Alg/(PEI-PEG/ $\alpha$ -CD/ $\text{Fe}_3\text{O}_4$ ) and Alg/ $\text{Fe}_3\text{O}_4$  film were 0.93% and 6.02%, (Fig.S7) indicating that

the Alg/(PEI-PEG/ $\alpha$ -CD/ $\text{Fe}_3\text{O}_4$ ) was much more homogenous. SEM measurement also showed that the PEI-PEG/ $\alpha$ -CD/ $\text{Fe}_3\text{O}_4$  particles were evenly distributed on the surface of Alg/(PEI-PEG/ $\alpha$ -CD/ $\text{Fe}_3\text{O}_4$ ) film. (Figure S8)

The Alg/(PEI-PEG/ $\alpha$ -CD/ $\text{Fe}_3\text{O}_4$ ) film showed significantly response to magnetic field. As shown in Fig. 3a, a free-standing Alg/(PEI-PEG/ $\alpha$ -CD/ $\text{Fe}_3\text{O}_4$ ) film (15 mm long and 5 mm wide), fixed at one edge on a filter paper. It was almost flat without the external magnetic field. But after putting a magnet near the film, the film bended to magnet nearly 180 $^\circ$ . The reaction to an applied magnetic field was very fast and reversible. The film can bend 180 $^\circ$  or return to its original shape within 6s with or without magnetic field (magnetic flux density of the permanent magnet was 0.4 tesla and the distance between magnet and film was 10 mm). The magnetization of curve of Alg/(PEI-PEG/ $\alpha$ -CD/ $\text{Fe}_3\text{O}_4$ ) film was a characteristic sigmoidal shape (Fig. S9), indicating the film was superparamagnetic.

The excellent magnetic-responsive property of the free-standing Alg/(PEI-PEG/ $\alpha$ -CD/ $\text{Fe}_3\text{O}_4$ ) film was further explored to build walking devices. The walking device was composed of Alg/(PEI-PEG/ $\alpha$ -CD/ $\text{Fe}_3\text{O}_4$ ) actuator and two pieces of polystyrene (PS) as claws at the opposite ends of the film (Fig. 4a). As shown in Fig. 4b, placing a paper or transparency above the device, the device bent upward into an arch with the external magnetic field due to the magnetic attraction. Switching off the magnetic field, the device unbent. This magnetic-responsive bending/unbending of device could convert to a one-directional motion on a ratchet substrate. With alternation of magnetic field and non-magnetic field, the device repeatedly bent and unbent, resulting in the forward motion of the device, while sliding backwards was prevented by the teeth of the ratchet (Figure 4c and Supporting Information, Movie 1). The velocity and control capacity are among the most important characteristics of a walking device. The walking velocity of this magnetic device can be controlled by changing the switching rate of magnetic field. The switching on/off magnetic field can be easily realized by turning on/off current. Comparing with other walking devices driven by humidity, photo, temperature or oscillating reaction, this walking device can move faster and easy to be controlled.

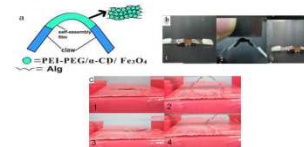


**Fig. 4** (a) Configuration of the walking device composed of the Alg/(PEI-PEG/ $\alpha$ -CD/ $\text{Fe}_3\text{O}_4$ ) actuator and two claws. (b) Bending and unbending of the walking device with alternation of magnetic field and non-magnetic field. (c) Motion of the walking device on a wrapping paper ratchet substrate with alternation of magnetic field and non-magnetic field. The film is 15 mm long and 5 mm wide. The claws are 7 mm wide and 20 mm long.

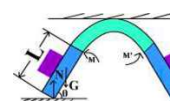


**Fig. 5** Schematic illustration of the equilibrium forces for the walking device with a load with magnetic field.

This magnetic walking device can be used for cargo transportation. We assumed that the magnetic field was strong enough, then, the maximum load-carrying capacity was relative to the Young's modulus of Alg/(PEI-PEG/ $\alpha$ -CD/Fe<sub>3</sub>O<sub>4</sub>) actuator.

Fig. 5 showed the schematic illustration of the equilibrium forces for the walking device with a load with magnetic field. It can be seen that, in a magnetic field, the devices bent and the hind claw was fixed by indentations on the ratchet surface. The contact point of the hind claw with the substrate served as a pivot point during each upward arching of the devices. Here,  $G$  denoted the gravity of the sum of gravity and load burden on the hind claw per unit width, and passed the midpoint of the claw.  $N$  was a support force from the underlying substrate. The bending moment ( $M$ ) produced by  $G$  and  $N$  can be described below:

$$M = G \frac{L}{2} \cos \theta \quad (1)$$

where  $L$  denoted the length of the claw, and the  $\theta$  was angle between the claw and the substrate surface. We assumed that the Alg/(PEI-PEG/ $\alpha$ -CD/Fe<sub>3</sub>O<sub>4</sub>) actuator can not be attracted to upward anymore in the magnetic field when loading was beyond maximum. Then, when the device carried the maximum, the  $\theta$  can be written as follows:

$$\theta = \arcsin \frac{H}{L + \frac{L}{2}} \quad (2)$$

where  $H$  was the distance between the transparent and substrate. The bending moment produced by  $G$  and  $N$  is in equilibrium with the bending moment  $M'$  imposed by Alg/(PEI-PEG/ $\alpha$ -CD/Fe<sub>3</sub>O<sub>4</sub>) actuator. On the basis of beam theory,<sup>5</sup> the  $M'$  can be expressed as following equation:

$$M' = \frac{1}{\rho} EI \quad (3)$$

where  $1/\rho$  is the curvature of actuator,  $E$  is the Young's modulus,  $I$  is the area moment of inertia.  $EI$  represents the flexural rigidity of the actuator. Here,  $I$  is

$$I = \frac{h^3}{12} \quad (4)$$

where  $h$  is the thickness of Alg/(PEI-PEG/ $\alpha$ -CD/Fe<sub>3</sub>O<sub>4</sub>) actuator.  $1/\rho$  can be written as:

$$\frac{1}{\rho} = \frac{2\theta}{l'} \quad (5)$$

Where  $l'$  denotes the length of the Alg/(PEI-PEG/ $\alpha$ -CD/Fe<sub>3</sub>O<sub>4</sub>) actuator after bending. We assumed that the  $l'$  was approximately equal to the original length  $l$  of actuator.

Because  $M$  is equilibrium with  $M'$ , we obtain the following equation:

$$G_{\max} = Eh^3 \frac{\theta}{3l \cos \theta} \quad (6)$$

$G_{\max}$  is the maximum load-carry capacity of one claw in a strip with unit width, therefore, the maximum load-carrying capacity for the walking device with width  $d$  is expressed as:

$$F_{\max} = 2dG_{\max} = 2dEh^3 \frac{\theta}{3l \cos \theta} \quad (7)$$

The length, thickness and the Young's modulus of the actuator were 15 mm, 0.04 mm and 80.84 MPa, respectively. The distance between the transparent and substrate  $H$  was 1.4 cm. The claws had a length  $L$  of 20 mm. The actuator and the claws were the same width  $d$  of 5 mm.

From the equ.(7), we can deserve that the maximum load-carrying capacity for the magnetic walking device is 2.043 mN. Experimental observation demonstrated that walking device with a 2.069 mN load walked clumsy and slowly, which agreed very well with the theoretical result and about 11 times heavier than the actuator. Furthermore, we measured the actual force generated by the films in the magnetic field, which was about 3.035 mN. (Detail measurement was provide in Supporting Information)

## Conclusions

In summary, we have successfully fabricated an magnetic active film by LBL self-assembly. This film showed superparamagnetic property and could act as a powerful actuator in a walking device. With alternation of magnetic field and non-magnetic filed, the device repeatedly bent and unbent, resulting in the inchworm-like motion on a ratchet substrate. This magnetic-driven walking device showed good transportation capability and easy to control the velocity because the on/off control of magnetic field is easy to realize.

## Acknowledgements

This work was funded by the National Natural Science Foundation of China (Grant no. 51373174), the CAS Knowledge Innovation Program (Grant no. KSCX2-EW-J-22), the West Light Foundation of CAS and Program for Changjiang Scholars, and the Innovative Research Team in University of Ministry of Education of China (IRT1026).

## Notes and references

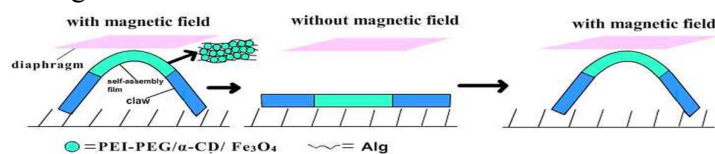
- <sup>a</sup> State Key Laboratory of Polymer Materials Engineering Polymer Research Institute of Sichuan University, Chengdu 610065 (China). Fax: (+86) 028-85403421; E-mail: zslbj@163.com
- <sup>b</sup> Chengdu Institute of Biology, Chinese Academy of Science, Chengdu, China, E-mail: libj@cib.ac.cn
- † Electronic Supplementary Information (ESI) available: Experimental section and supplementary figures and movies. See DOI: 10.1039/b000000x/
- 1 (a) S. Y. Dong, Y. Luo, B. Zheng, X. Ding, Y. H. Yu, Z. Ma, Q. L. Zhao, F. H. Huang, *Angew. Chem. Int. Ed.*, 2011, **50**, 1905-1909; (b) X. Z. Yan, D. H. Xu, X. D. Chi, J. Z. Chen, S. Y. Dong, X. Ding, Y. H. Yu, F. H. Huang, *Adv. Mater.*, 2012, **24**, 362-369; (c) M. M. Zhang, D. H. Xu, X. Z. Yan, J. Z. Chen, S. Y. Dong, B. Zheng, F. H.



- Huang, *Angew. Chem. Int. Ed.*, 2012, **51**, 7011-7015; (d) Y. Yu, M. Nakano, T. Ikeda, *Nature*, 2003, 425, 145.
- 2 (a) F. Ilievski, A. D. Mazzeo, R. F. Shepherd, X. Chen and G. M. Whitesides, *Angew. Chem.*, 2011, **123**, 1930-1935; (b) W. B. Sherman, N. C. Seeman, *Nano Lett.*, 2004, **4**, 1203-1207; (c) R. A. Delden, M. K. J. Wiel, M. M. Pollard, J. Vicario, N. Koumra, *Nature*, 2005, **437**, 1337-1340.
- 3 T. Fukushima, K. Asaka, A. Kosaka and T. Aida, *Angew. Chem.*, 2005, **117**, 2462-2465.
- 10 4 (a) M. You, Y. Chen, X. Zhang, H. Liu and R. Wang, *Angew. Chem.*, 2012, **124**, 2507-2510; (b) S. Ahir and E. M. Terentjev, *Nat. Mater.*, 2005, **4**, 491-495; (c) P. Poosanaas, K. Tonooka, K. Uchino, *Mechatronics*, 2000, **10**, 467-487; (d) Y. Yu and T. Ikeda, *Angew. Chem. Int. Ed.*, 2006, **45**, 5416-5418; (e) M. Yamada, M. Kondo, J. Mamiya, Y. Yu, M. Kinoshita, C. J. Barrett and T. Ikeda, *Angew. Chem. Int. Ed.*, 2008, **47**, 4986-4988.
- 15 5 S. Maeda, Y. Hara, T. Sakai and R. Yoshida, *Adv. Mater.*, 2007, **19**, 3480-3484.
- 6 Y. Ma, Y. Y. Zhang, B. S. Wu, W. P. Sun, Z. G. Li and J. Q. Sun, *Angew. Chem.*, 2011, **123**, 6378-6381.
- 20 7 (a) K. A. Arteaga, A. A. Rodriguez and E. Barrado, *Anal. Chim. Acta*, 2010, **674**, 157-165; (b) P. Howes, M. Green, A. Bowers, D. Parker, G. Varma, M. Kallumadil, M. Hughes, A. Warley, A. Brain and R. Botnar, *J. Am. Chem. Soc.*, 2012, **132**, 9832-9842.
- 25 8 R. Fuhrer, E. K. Athanassiou, N. A. Luechinger and W. J. Stark. *Small*, 2009, **5**, 383-388.
- 9 (a) K. G. Gopchandran, B. Joseph, J. T. Abraham, P. Koshy and V. K. Vaidyan, *Vacuum*, 1997, **48**, 547-550; (b) M. Endo, S. Kanai, S. Ikeda, F. Matsukura and H. Ohno, *Appl. Phys. Lett.*, 2010, **96**, 212503; (c) S. J. An, Y. Zhu, S. H. Lee, M. D. Stoller, T. Emilsson, S. Park, A. Velamakanni, A. An and R. S. Ruoff, *J. Phys. Chem. Lett.*, 2010, **1**, 1259-1263; (d) M. C. Leon, E. Coronado, A. L. Munoz, D. Repetto, L. Catala and T. Mallah, *Langmuir*, 2012, **28**, 4525-4533; (e) M. Zhang, Y. Yan, K. Gong, L. Mao, Z. Guo and Y. Chen, *Langmuir*, 2004, **20**, 8781-8785; (f) X. Zhang, H. Chen and H. Zhang, *Chem. Commun.*, 2007, 1395-1405; (g) A. A. Mamedov and N. A. Kotov, *Langmuir*, 2000, **16**, 5530-5533.
- 30 10 (a) F. H. Huang, H. W. Gibson, *Prog. Polym. Sci.*, 2005, **30**, 982-1018; (b) X. Z. Yan, F. Wang, B. Zheng, F. H. Huang, *Chem. Soc. Rev.*, 2012, **41**, 6042-6065; (c) G. C. Yu, X. Z. Yan, C. Y. Han, F. H. Huang, *Chem. Soc. Rev.*, 2013, **42**, 6697-6722.
- 35 11 (a) X. W. Meng, J. Qin, Y. Liu, M. M. Fan, B. J. Li, S. Zhang and X. Q. Yu, *Chem. Commun.*, 2010, **46**, 643-645; (b) W. Ha, X. W. Meng, Q. Li, M. M. Fan, S. L. Peng, L. S. Ding, X. Tian, S. Zhang and B. J. Li, *Soft Matter*, 2010, **6**, 1405-1408; (c) M. M. Fan, X. Zhang, J. Qin, B. J. Li, S. Sun and S. Zhang, *Macromol. Rapid Commun.*, 2011, **31**, 1533-1538; (d) C. Cheng, X. J. Han, Z. Q. Dong, Y. Liu, B. J. Li and S. Zhang, *Macromol. Rapid Commun.*, 2012, **32**, 1965-1971. (e) W. Ha, H. Wu, Y. Ma, M. M. Fan, S. L. Peng, L. S. Ding, S. Zhang, B. J. Li, *Carbohydr. Polym.*, 2013, **92**, 523-528; (f) X. W. Meng, W. Ha, C. Cheng, Z. Q. Dong, L. S. Ding, B. J. Li and S. Zhang, *Langmuir*, 2011, **27**, 14401-14407; (g) Q. Li, B. Xia, M. Branham, W. Ha, H. Wu, S. L. Peng, L. S. Ding, B. J. Li and S. Zhang, *Carbohydr. Polym.*, 2011, **86**, 120-126.
- 55

## Layer-by-Layer Self-assembly Films for Building Magnetic Driven Walking Devices

Hong-Su Zhang,<sup>a</sup> Ling Luo,<sup>a</sup> Ge Fang,<sup>b</sup> Wan-Zhen Zhang,<sup>a</sup> Bang-Jing Li<sup>\*b</sup> and Sheng Zhang<sup>\*a</sup>



In this paper, we fabricated a magnetic-driven walking device comprising magnetic active layer-by-layer film. Alternating the magnetic fields, the device walked steadily and fast on the substrate like an inchworm, and showed good transportation capability.